Pacific Northwest National Laboratory
Operated by Battelle for the U.S. Department of Energy

Battelle . . . Putting Technology To Work

Adventures of Spinel Crystals in a High-Level Waste Glass Melter

Pavel Hrma, Jesse Alton, Alexandr Franěk,[§] Pavel Izák, Antonín Jiřička, Jaroslav Kloužek,[†] Martin Míka,[†] Lubomír Němec,[‡] Trevor Plaisted, Petr Schill,[§] and Benjamin Wilson

[†]Institute of Chemical Technology, Prague, Czech Republic, [‡]Academy of Sciences, Prague, Czech Republic
[§]Glass Service, Inc., Vsetín, Czech Republic

Abstract

Constraining HLW glass from precipitating spinel crystals in the melter limits waste loading. Even a few percent increase in waste loading translates into billions of dollars in savings, thus there is strong economic incentive to establish bounds of tolerable spinel formation provided melter performance is not adversely affected. Acceptable fraction of spinel in molten glass has been assessed at values from 0 to 1 mass%, but the real value depends on the melter type, the size and number density of spinel crystals, the temperature and velocity fields in the melter, and the spinel sludge rheology. These factors are being investigated by means of mathematical modeling.

Spinel crystals form already during the initial melting stages, precipitating from the nitrate melts within the bed of reacting melter feed. Spinel formation starts at temperatures above 400ºC and peaks at 650ºC, the temperature at which the nitrate decomposition is nearly complete and glass-forming melt is established. Though these crystals usually dissolve in the glass-forming melt during the final stages of conversion, spinel forms again when the temperature of molten glass drops below the liquidus temperature.

The temperature history of the melt in the HLW glass melter is rather wild. A spinel crystal may undergo several cycles of dissolution and growth before reaching its final destination either in the glass canister or at the melter bottom. The number density of spinel crystals depends on the concentration of some minor waste components, such as RuO_2 and Ag_2O, and may vary from 1 to 10^4 crystals per mm^3. As a result, spinel crystal size varies from 1 to 100 µm. Laboratory studies of spinel formation must consider that spinel crystallization is a strong function of the temperature history and that surface crystallization may affect crystallization kinetics in powdered glass.

The rates of crystal growth and dissolution depend on melt temperature and on the crystal number density which in turn is determined by the presence of heterogeneous nuclei provided by some minor waste components. The rate of spinel growth and dissolution has been measured under conditions that simulate the temperature history in the melter. At temperatures at which crystals move by buoyancy force, the rate of growth and dissolution is constant at constant temperature and exhibits an Arrhenius dependence on temperature.

Understanding the complex behavior of spinel under the conditions of glass melting, including redox, is important for the development of mathematical models of spinel settling in the HLW glass melter and for the optimization of HLW glass with respect to the cost of the product and the risk for melter operation. The mathematical model for the waste glass melter with spinel settling has recently been developed. The behavior of spinel in molten glass was also studied using physical modeling. Crucible melts were performed to learn about the mode of spinel settling.

1. Spinel

The most common crystalline phase that precipitates from HLW glasses at temperature (T) > 1050°C is spinel (Figures 1-1 and 1-2). Figure 1-3 displays spinel composition in MS-7 glass (see Table I) as a function of temperature.

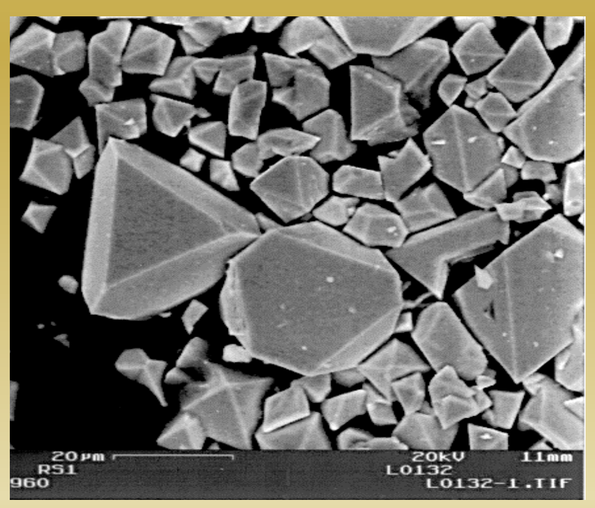

Figure 1-1. Spinel crystals from a HLW glass (SEM)

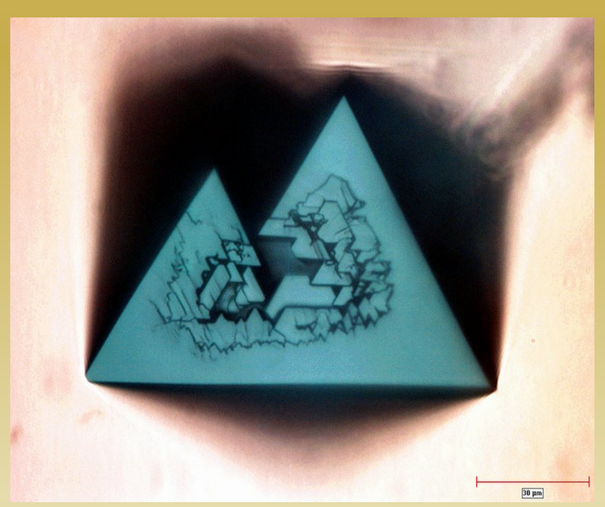

Figure 1-2. A spinel crystal twin from a HLW glass (optical microscope)

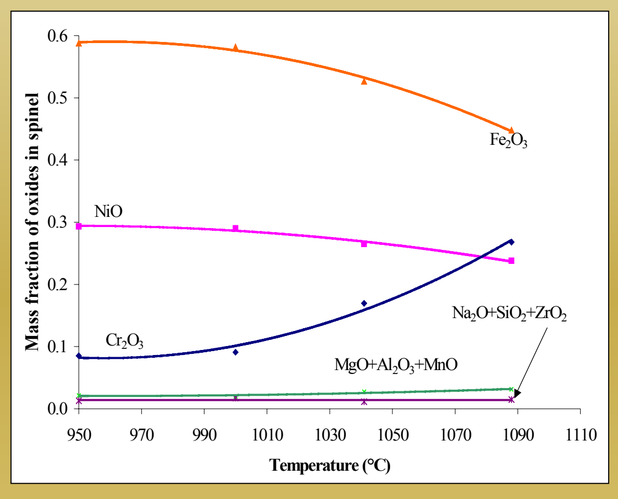

Figure 1-3. Spinel composition vs. T (SEM EDS)

Just below liquidus temperature (T_L), spinel contains more Cr_2O_3 (by mass) than NiO. As temperature decreases, trevorite ($NiFe_2O_4$) becomes the dominant component. Other oxides are either minor components of spinel (MnO, and possibly MgO and Al_2O_3) or inclusions (Na_2O, SiO_2, and ZrO_2). Glass inclusions are likely to be trapped in rapidly growing crystals (Figure 1-2).

2. Feed-to-glass conversion

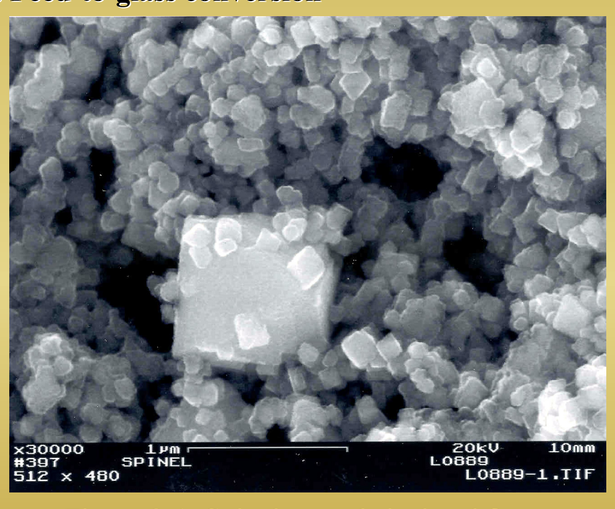

Figure 2-1. Spinel crystals isolated from HLW feed (650°C, SEM)

Spinel is one of the intermediate crystalline compounds that form during the feed melting reactions (Figure 2-1). The main HLW feed melting reaction is that between nitrates and silica at 650°C to 750°C (Figures 2-2 and 2-3). Spinel and sodalite precipitate from the nitrate melt and later dissolve in the glass-forming melt (Figure 2-3). Feed expands as soon as the glass-forming melt becomes interconnected. The cause of the expansion is probably $NO+O_2$ from sodalite (Figure 2-2).

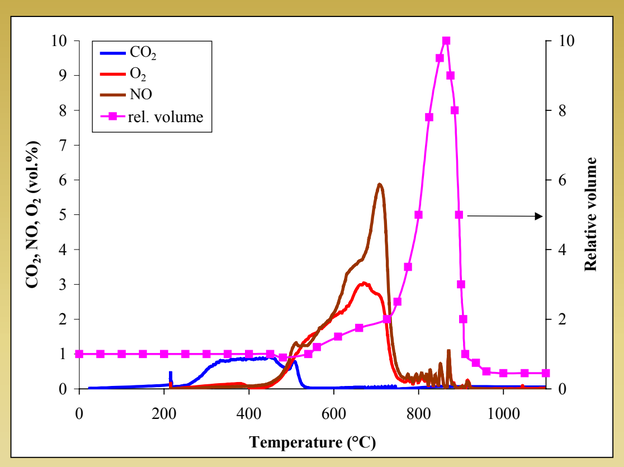

Figure 2-2. Evolved gas composition and feed volume expansion (4°C/min)

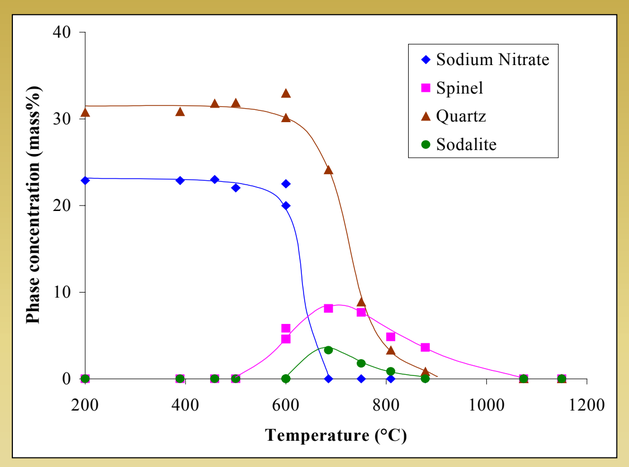

Figure 2-3. Phase concentration in MS-7 feed vs. T at 4°C/min

3. Equilibrium

The spinel equilibrium fraction (C_o) depends on T as

$$C_o = C_{\max}\left\{1-\exp\left[-B_L\left(\frac{1}{T}-\frac{1}{T_L}\right)\right]\right\} \qquad (3\text{-}1)$$

where T_L is the liquidus temperature, and C_{max} and B_L are composition-dependent coefficients. This relationship is displayed in Figure 3-1 for glasses of varied composition of the MS-7 baseline glass (Tables I).

Table I. MS-7 (baseline) glass composition and component variations (in mass fractions)

Component	Al_2O_3	Cr_2O_3	Fe_2O_3	Li_2O	MgO	Na_2O	NiO	B_2O_3	MnO	SiO_2	ZrO_2
High	0.110	0.005	0.150	0.060	0.030	0.180	0.018	-	-	-	-
Baseline	0.080	0.003	0.115	0.045	0.006	0.153	0.010	0.070	0.005	0.453	0.060
Low	0.050	0.001	0.080	0.030	0.000	0.120	0.003	-	-	-	-

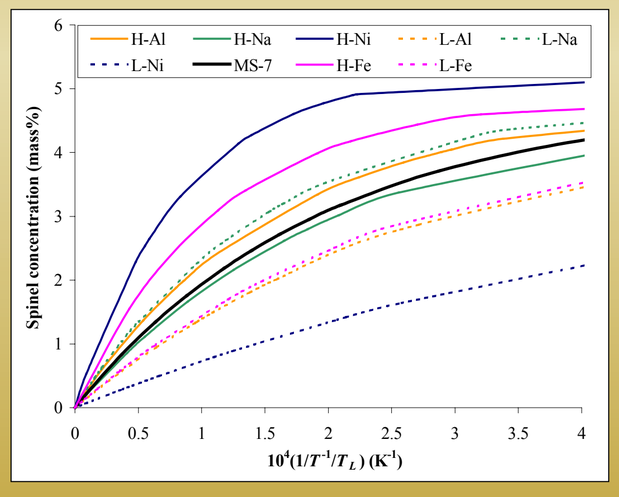

Figure 3-1. Equilibrium fraction of spinel in glasses with varied components (Table I) vs. ($1/T$-$1/T_L$)

The difference between T_L and the temperature at which an acceptable $C_o = C_{acc} << 1$ is

$$\Delta T = \frac{T_L^2}{C_{\max} B_L} C_{acc} \qquad (3\text{-}2)$$

Figure 3-2 shows T_L, C_{max}, B_L, and ΔT (C_{acc} = 0.01) vs. change in glass composition (Δg_i is the i-th component addition to baseline glass).

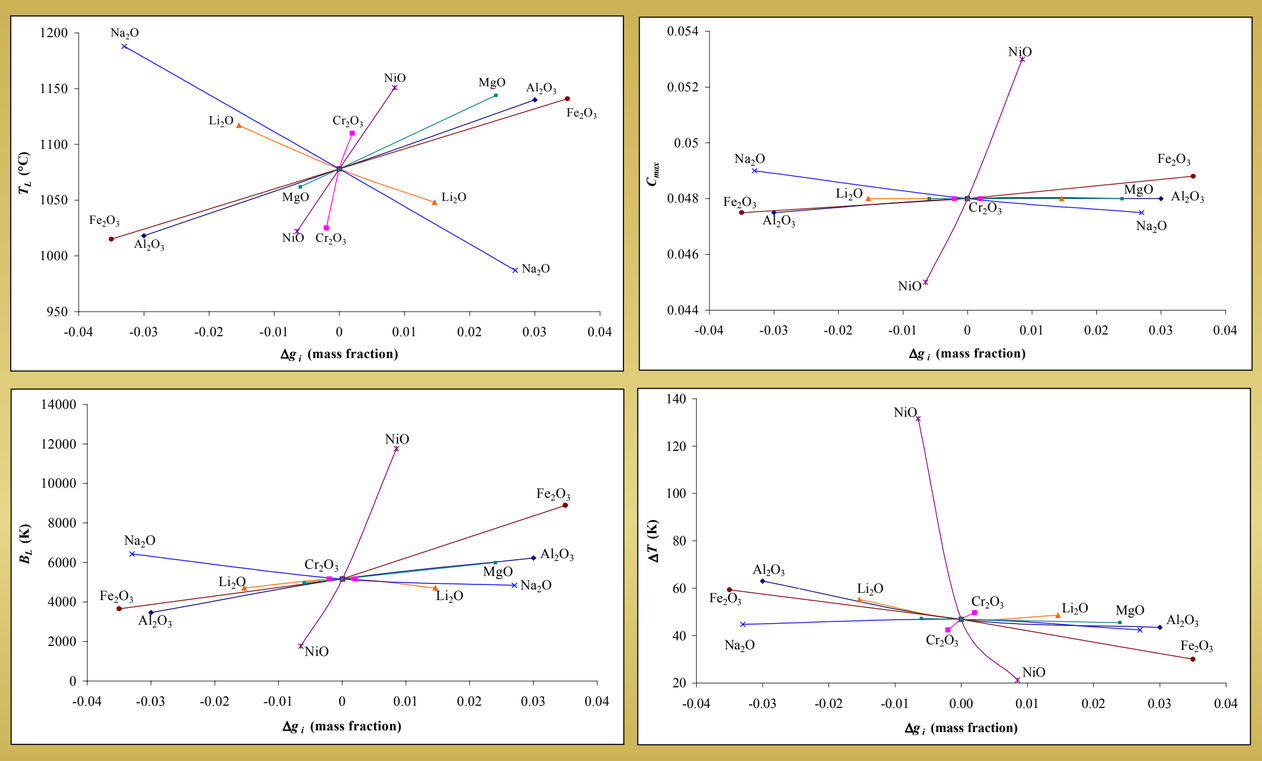

Figure 3-2. Effect of glass composition on the equilibrium coefficients T_L, C_{max}, B_L, and ΔT (C_{acc} = 0.01) [Equations (3-1) and (3-2)]

4. Effect of temperature history

For a glass without nucleation agents, crystal number density depends on the temperature history. Figure 4-1 shows the number of spinel crystals formed at 950°C as a function of the nucleation temperature.

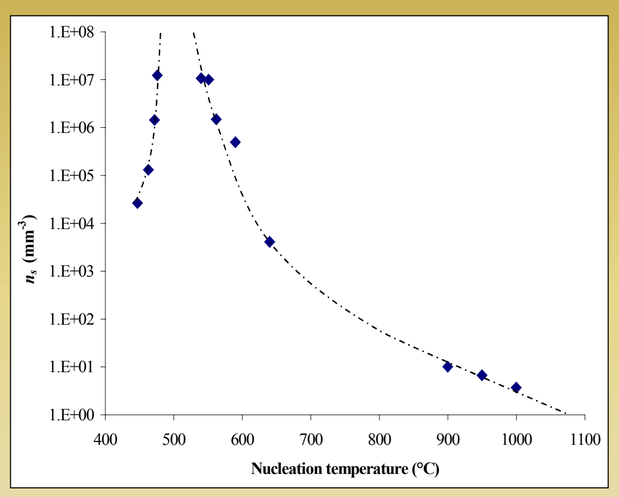

Figure 4-1. Crystal number density vs. nucleation temperature (T_N)

5. Effect of minor components

Minor components (called Others) do not have a dramatic effect on spinel equilibrium (Figure 5-1), but have a profound impact on spinel crystallization kinetics (Figure 5-2). This is because Others provide heterogeneous nuclei for spinel crystals. The number density (n_s) of crystals in glass is plotted versus time in Figure 5-3, which shows that n_s is independent of the heat-treatment time. The average log (n_s) values are plotted as a function of Others concentration in Figure 5-4.

As Figure 5-4 shows, adding 1 mass% Others increases n_s by approximately 3.2 times from the baseline glass (0 mass%). This change can be attributed to heterogeneous nucleation caused by noble metals (RuO_2 and possibly Rh). Further additions of Others have little effect on n_s until the mass fraction of Others reaches 4 mass%. This level increases n_s nearly 500 times compared to 0% Others. We may attribute this dramatic effect to the precipitation of Ag-Cu colloids whose presence is evident from the rainbow-like opalescence of the glass.

Spinel crystal growth is diffusion-controlled. Equilibrium concentration of spinel in glass is reached sooner if the number density is higher (the higher n_s, the smaller the glass volume per crystal). Therefore, the rate coefficient (k) increases as n_s increases (Figure 5-5). The crystal size, plotted in Figure 5-6 as a function of time for samples heat-treated at T = 950°C, decreases with increasing n_s.

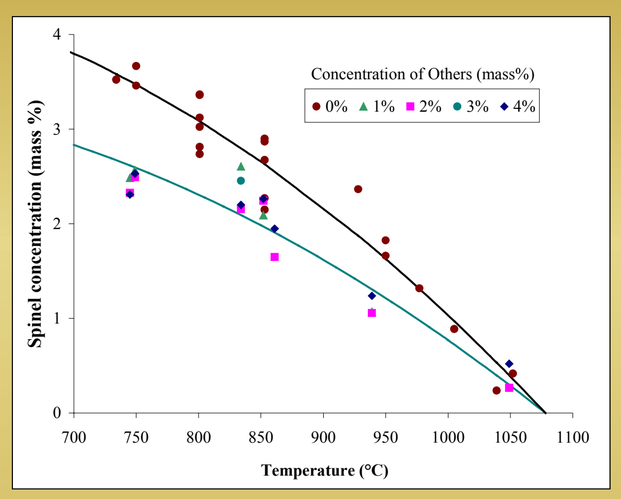

Figure 5-1. Equilibrium fraction of spinel vs. T and Others mass fraction

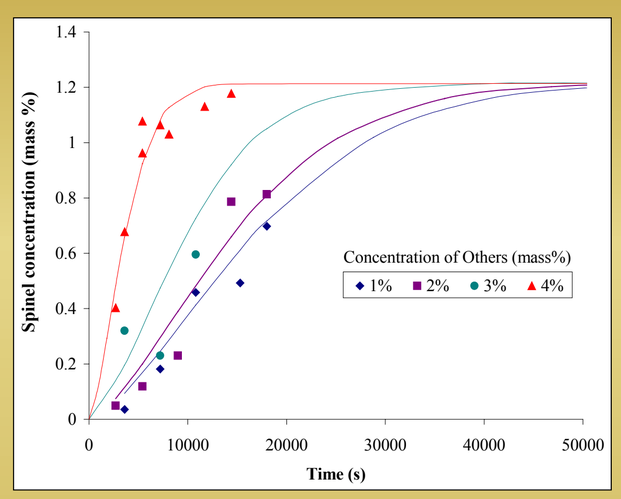

Figure 5-2. Spinel concentration vs. time and Others mass fraction at 950°C

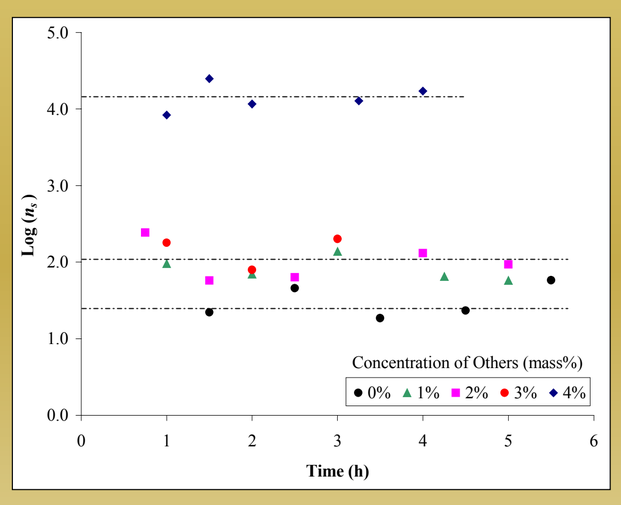

Figure 5-3. Log (n_s) vs. time

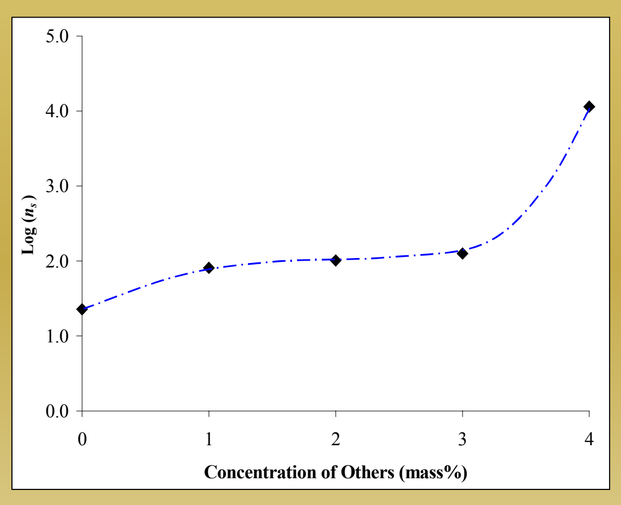

Figure 5-4. Log (n_s) vs. % Others

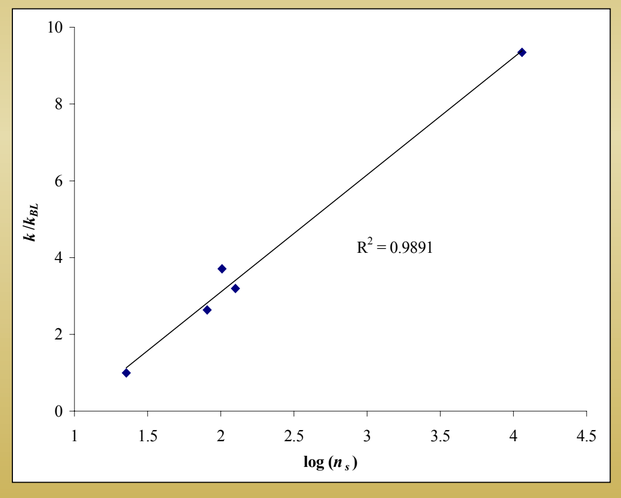

Figure 5-5. k/k_{BL} vs. log(n_s); the subscript BL stands for baseline (glass with 0% Others)

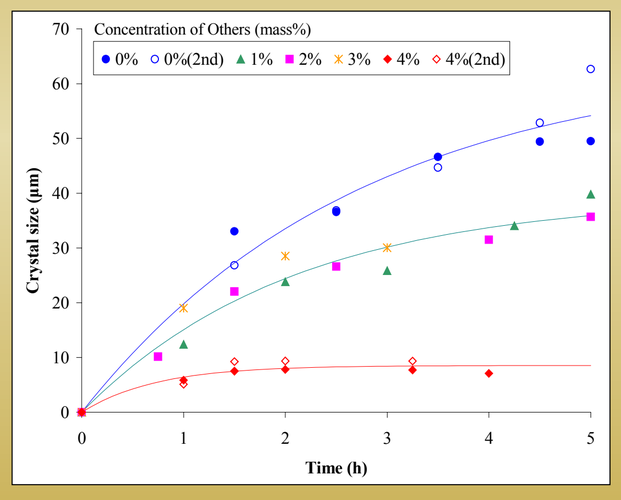

Figure 5-6. Spinel crystal size as a function of time and Others mass fraction

6. Crystal dissolution (in progress)

Spinel crystals were created by heat-treating MS-7 glass at 900°C. Crystals dissolve if $C > C_0$, where C is the spinel mass fraction in molten glass (subscript 0 stands for equilibrium). Figure 6-1 shows the crystal size decrease at constant temperature. The initial rate of dissolution is an Arrhenius function of inverse temperature (Figure 6-2), i.e.,

$$u_{diss} = u_0 \exp\left(-\frac{B_{diss}}{T}\right) \qquad (6\text{-}1)$$

where u_{diss} is the dissolution rate and B_{diss}= 52,183 K is the apparent activation energy ($u_{diss} = \partial a/\partial t$; here a is the spinel crystal size).

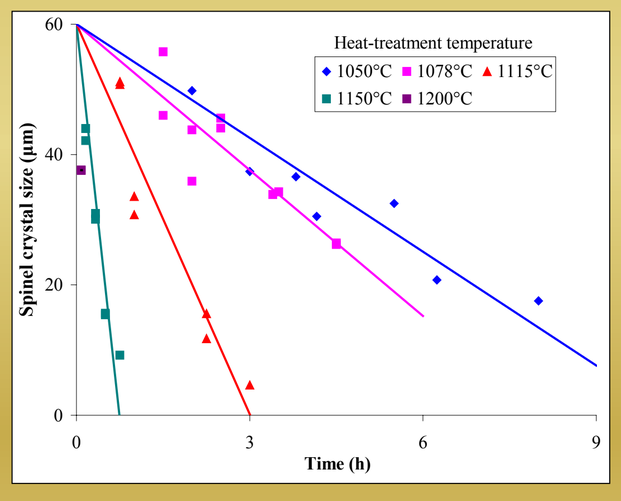

Figure 6-1. Spinel crystal size vs. time and temperature

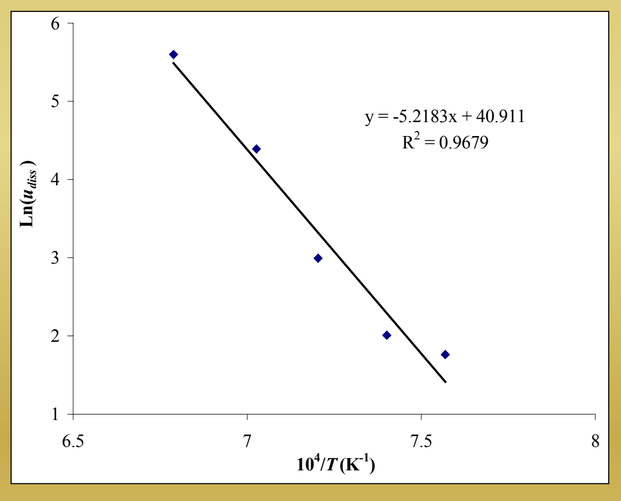

Figure 6-2. Arrhenius plot for spinel dissolution rate

Equation (6-1) is only a fitting function. In reality

$$u_{diss} = D\frac{\Delta c}{\delta} \qquad (6\text{-}2)$$

where D is the diffusion coefficient, Δc is the concentration difference of dissolved spinel at the interface and the bulk, and δ is the concentration layer thickness. Note that $\Delta c \to 0$ as $T \to 900$°C. The settling rate of spinel crystals affects δ.

7. Crystal growth (in progress)

MS-7 glass was held at 1200°C for 30 minutes and then cooled to the heat-treatment temperature to precipitate spinel. Crystals grew while settling (Figure 7-1).

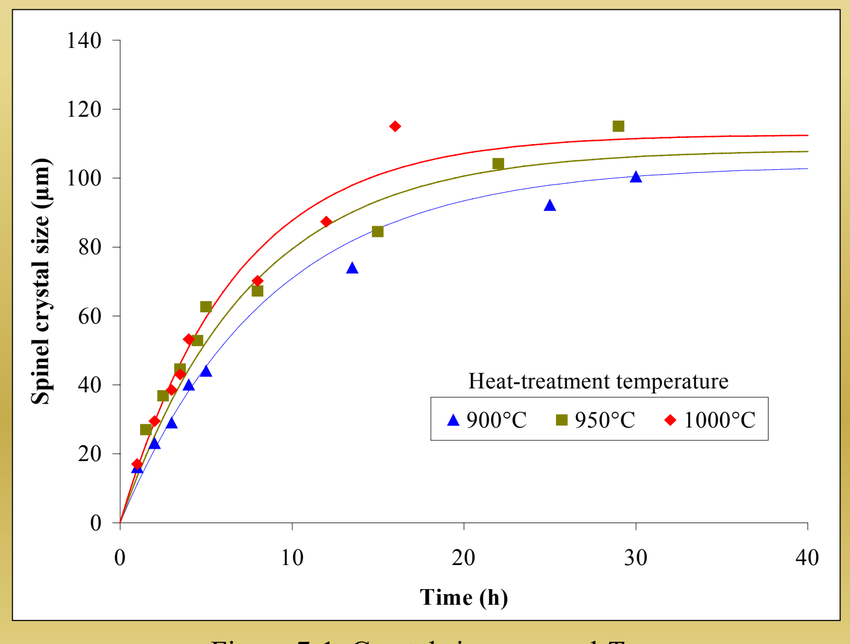

Figure 7-1. Crystal size vs. t and T

The lines in Figure 7-1 represent the function

$$a = a_0\left(1 - e^{-bt}\right) \qquad (7\text{-}1)$$

where a is the crystal size, $a_0 = \beta T$ (with β = 0.0885 µm/K) is the final crystal size, and $b = b_0 \exp(-B_{growth}/T)$ (with b_0 = 3.53 h^{-1} and B_{growth} = 4018 K) is the growth rate coefficient.

The final crystal size, the C_0 values, and the corresponding n_S values are:

T (°C)	a_0 (µm)	C_0	n_S (mm^{-3})
900	104	0.0217	10.1
950	108	0.0163	6.7
1000	113	0.0103	3.7

If room-temperature glass is isothermally heat-treated, spinel crystals are small (about 1µm) because of the large number of nuclei (Figure 4-1). These crystals grow rapidly (Figure 7-2).

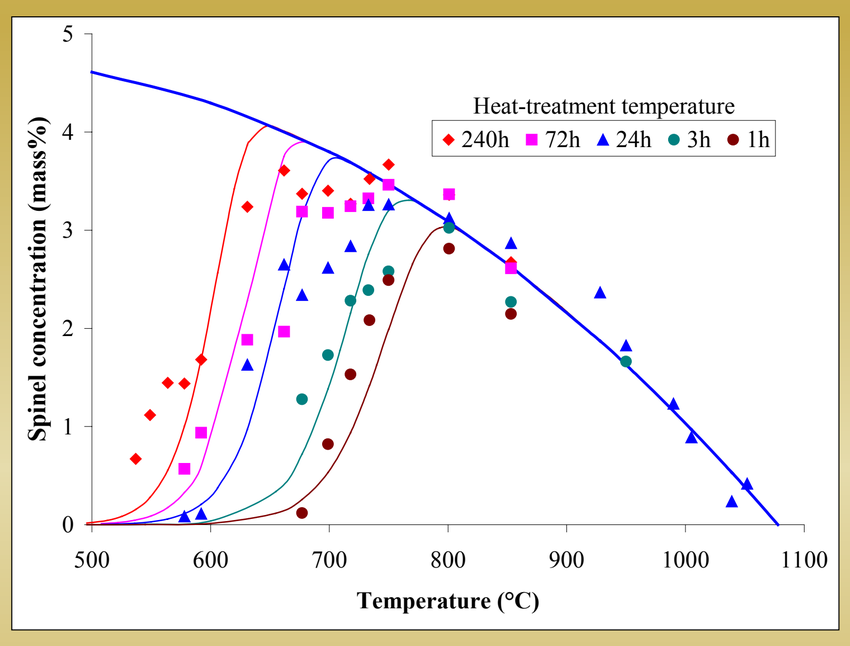

Figure 7-2. Avrami plot of spinel crystallization kinetics

Crystal growth and dissolution in the melter are subjected to a wild temperature history (Figure 7-3).

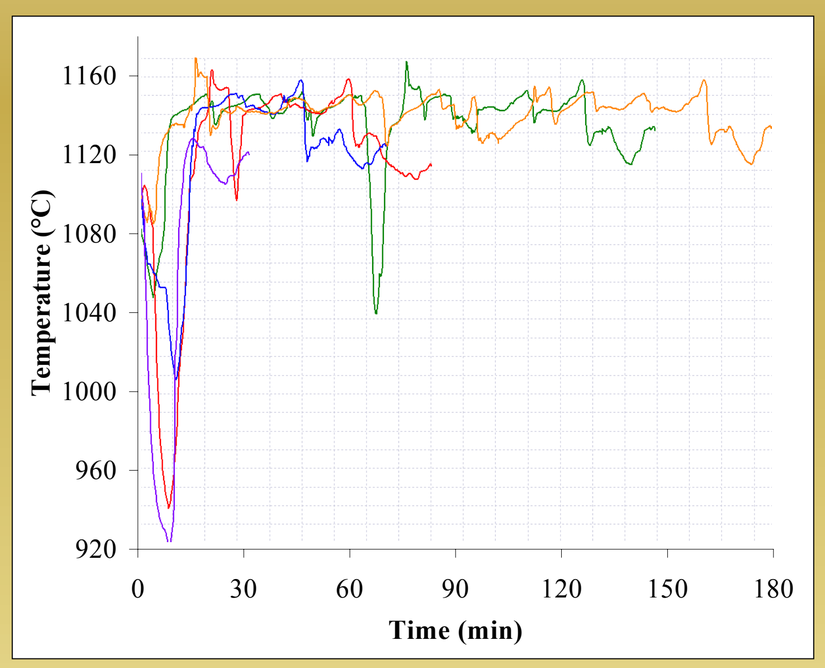

Figure 7-3. Temperature history of several material points of glass in a HLW glass melter

8. Surface crystallization

It is important to simulate the conditions under which spinel crystallizes in the melter. If a powdered glass is heat treated, surface crystallization occurs. The trends seen in Figures 8-1 and 8-2 cannot be extrapolated to higher temperatures. Surface crystallinity does not develop at temperatures above 950°C and no crystals exist above T_L at equilibrium.

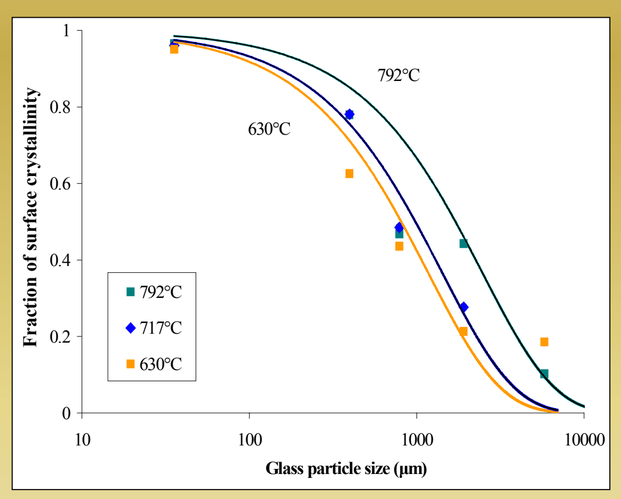

Figure 8-1. Fraction of surface crystallinity vs. glass particle size

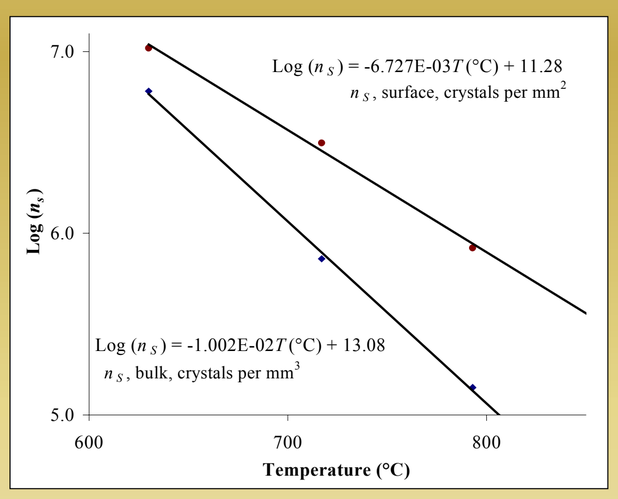

Figure 8-2. Average surface (per mm^2) and bulk (per mm^3) crystal number density vs. T

9. Redox

Ferrous-ferric ratio depends on the oxygen partial pressure (p_{O_2}) and temperature:

$$\log\frac{[Fe(II)]}{[Fe(III)]} = -\frac{1}{4}\log(p_{O_2}) + \frac{\Delta H_r}{2.303RT} + C \qquad (9\text{-}1)$$

Similar relationships can be written for Cr(VI)/Cr(III), Ni(0)/Ni(II), etc. Liquidus temperature for spinel phase is a function of p_{O_2} (Figure 9-1). At $10^{-9} < p_{O_2}$ (kPa) $< 10^2$, T_L increases as p_{O_2} decreases. The sharp T_L increase at $1 < p_{O_2}$ (kPa) $< 10^2$ is associated with the reduction of Cr(VI) to Cr(III). At the same time, until $p_{O_2} = 10^{-4}$ kPa, Fe(III) is being reduced to Fe(II). This change causes a milder increase in T_L at $10^{-4} < p_{O_2}$ (kPa) < 1. Within the interval $10^{-9} < p_{O_2}$ (kPa) $< 10^{-4}$, the majority of Ni(II) is reduced to Ni(0) while T_L only slightly increases. At $p_{O_2} < 10^{-9}$ kPa, T_L decreases with decreasing p_{O_2}, while Fe(II) is being reduced to Fe(0).

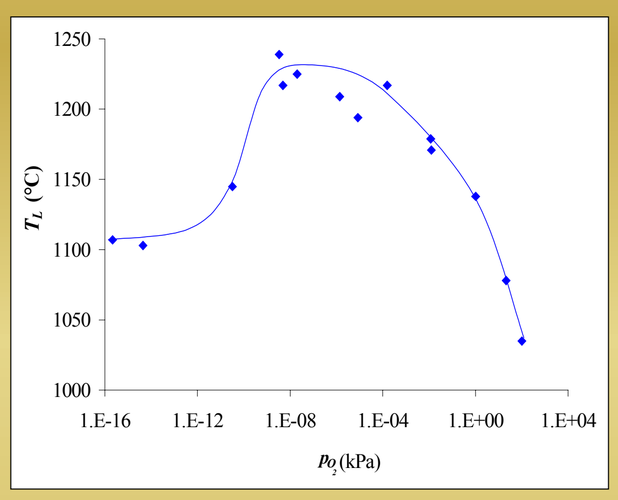

Figure 9-1. T_L vs. p_{O_2}

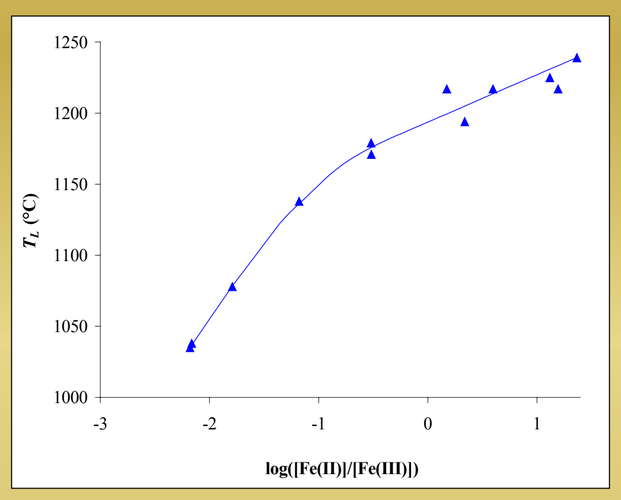

Figure 9-2. T_L vs. log([Fe(II)]/[Fe(III)])

10. Settling

In a laboratory crucible, spinel settling usually drives a single flow-cell (Figure 10-1). The depth of the settling front (h) increased in accordance with the modified Stokes law if the initial period of crystal growth was considered (Figure 10-2).

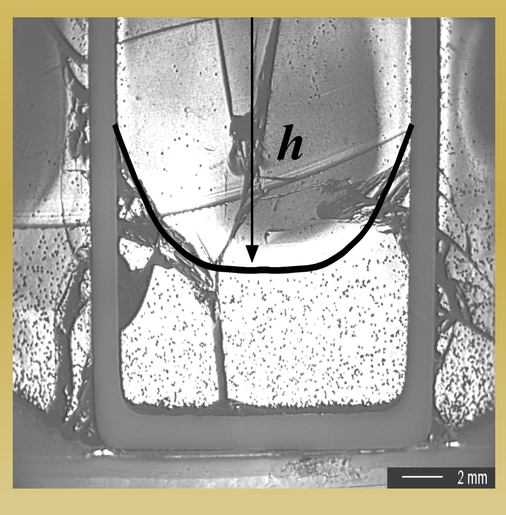

Figure 10-1. Spinel settling front in a crucible at 950°C for 23 h (MS-7 glass)

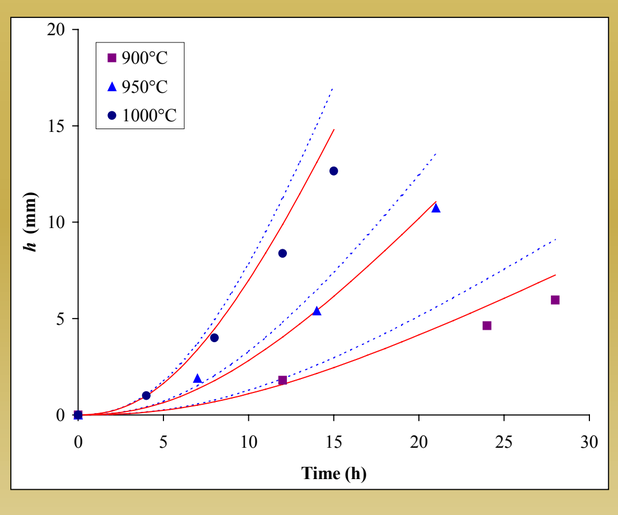

Figure 10-2. Settling front depth vs. t and T; measured and calculated by classical (blue line) and modified (red line) Stokes law

11. Spinel sludge rheology

Measurements were performed on a special HLW 10-component, RuO_2-free glass with T_L = 1344°C. Spinel sludge from this glass behaved as a rheopectic pseudoplastic liquid. Its shear stress (τ_{ef}) was an increasing function of velocity gradient (∇v_{ef}) and time. At constant T and ∇v_{ef}, the changes in sludge structure were causing a higher friction and increasing τ_{ef} with time (aging). The aging phenomenon was not observed at $T > 1300$°C. As ∇v_{ef} and T increased, the apparent viscosity (η_a) decreased as the sludge structure was rearranging. The sludge approached time-independent behavior above 1300°C. At 1094°C, η_a of the sludge from a similar glass with minor components added, including 0.03 mass% RuO_2, was roughly 20 times higher than that of RuO_2-free glass, but only 2 to 4 times higher at temperatures above 1300°C. Spinel crystals bonded with RuO_2 needles are shown in Figure 11-1.

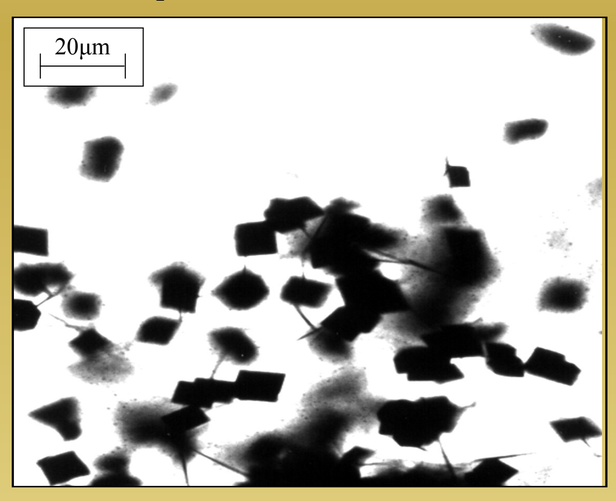

Figure 11-1. Spinel crystals bonded with RuO_2 needles

Publications

1. M. W. Stachnik, P. Hrma, and H. Li, "Effects of High-level Waste Glass Composition on Spinel Precipitation," *Ceramic Transactions* 107 (1999).
2. M. Mika, J. V. Crum, and P. Hrma, "Spinel Precipitation in High-Level Waste Glass," *Proceedings of the 5th ESG Conference,* Prague, Czech Republic 1999.
3. M. Mika, P. Hrma, and M. J. Schweiger, "Rheology of Spinel Sludge in Molten Glass," *Ceramics-Silikaty* (accepted).
4. P. Hrma: "Modeling of Spinel Settling in Waste Glass Melter." *In Science to Support DOE Site Cleanup*, Pacific Northwest National Laboratory, PNNL-12208 UC-2000 (1999).
5. P. Izak, P. Hrma, M.J. Schweiger, "Nonisothermal crystallization of spinel from a high-level waste feed," to be published in ACS proceedings.
6. P. Schill, and P. Vlcek: "Mathematical Model of Radioactive Waste Glass Melter," *5th International Seminar on Mathematical Simulation in Glass Melting Proceedings*, Horni Becva, Czech Republic, p. 112-118 (1999).
7. P. Schill, A. Franek, M. Trochta, P. Viktorin, and P. Vlcek: "Integrated Glass Furnace Model," *5th International Seminar on Mathematical Simulation in Glass Melting Proceedings*, Horni Becva, Czech Republic, p.125-137 (1999).
8. P. Hrma, J. D. Vienna, J. V. Crum, G. F. Piepel, and M. Mika, "Liquidus Temperature of High-Level Waste Borosilicate Glasses with Spinel Primary Phase," *Mat. Res. Soc. Proc.* (2000).
9. J. Klouzek, J. Alton, T.J. Plaisted, and P. Hrma, "Crucible Study of Spinel Settling in High-Level Waste Glass," *Ceramic Transactions* (to be submitted).
10. P. Izak, J. Klouzek, and P. Hrma, "Evolution of crystalline Phases during High-Level Waste Feed-to-Glass Conversion," *Ceramic Transactions* (to be submitted).
11. T.J. Plaisted*, J. Alton, P. Hrma, and B. Wilson, "Spinel Nucleation and Growth in High-Level Waste Glass," *Ceramic Transactions* (to be submitted).
12. P. Izak, P. Hrma, J. D. Vienna, and B. Wilson, "Effect of Oxygen Partial Pressure on Liquidus Temperature with Spinel Primary Phase," *Ceramic Transactions* (to be submitted).
13. T.J. Plaisted*, F. Mo, B. Wilson, and P. Hrma, Surface Crystallization of Spinel and Acmite in High-Level Waste Glass," *Ceramic Transactions* (to be submitted).
14. J. Klouzek and A. Franek, "Physical and Mathematical Modeling of Spinel Settling in High-Level Waste Glass," Waste Management 2000 Conference Proceedings (in print), Tucson, Arizona 2000.

12. Melter modeling

A HLW glass melter was modeled using the Glass Service GS-CAD model code (Figure 12-1). The temperature and flow in both cuts (cross and longitudinal) show the good mixing ability of this type of melter. A spinel settling model is being developed. A preliminary assessment of spinel distribution in the melter is shown in Figure 12-2.

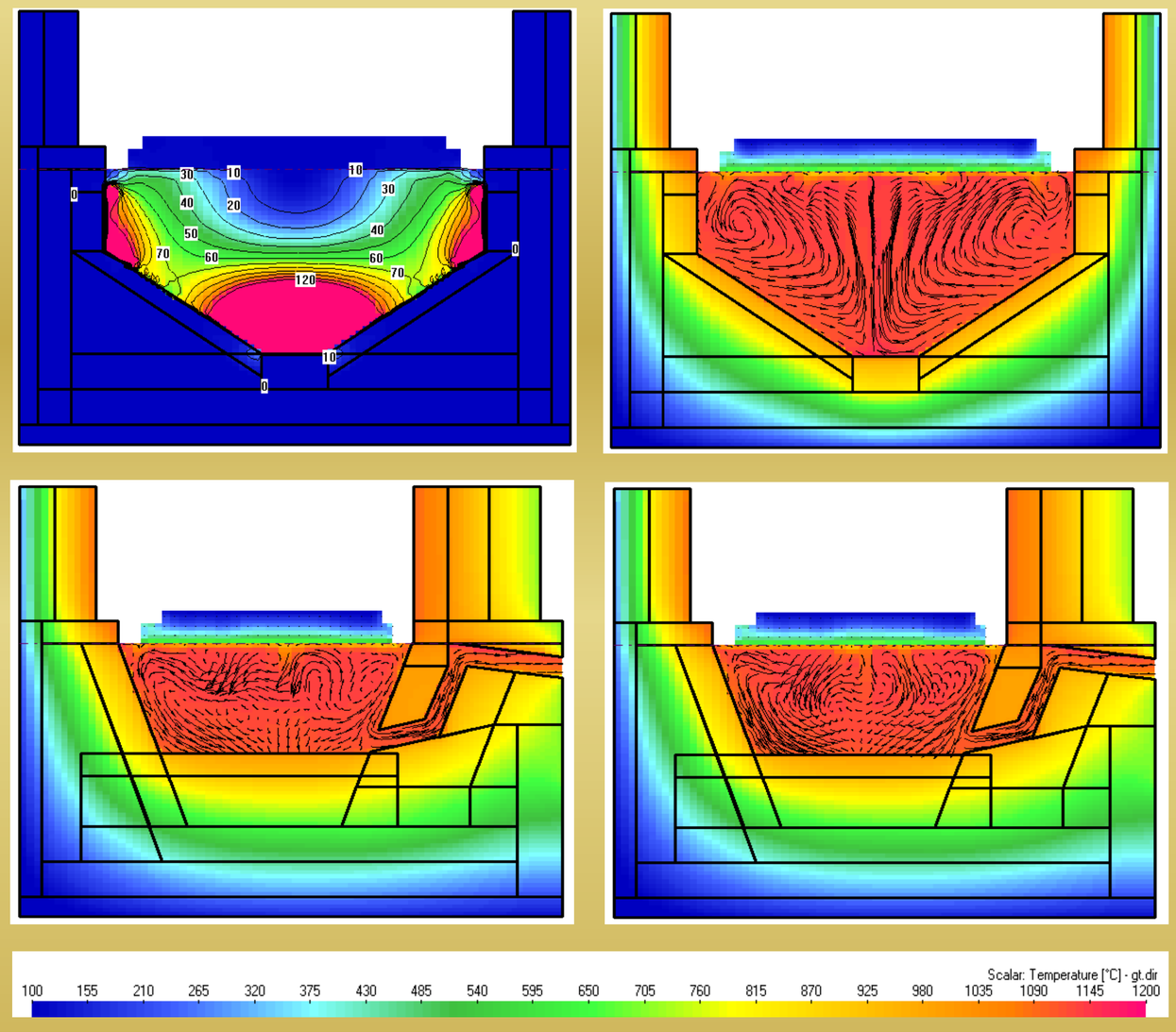

Figure 12-1. Electric (in kW/m^3), temperature, and flow fields in a HLW glass melter

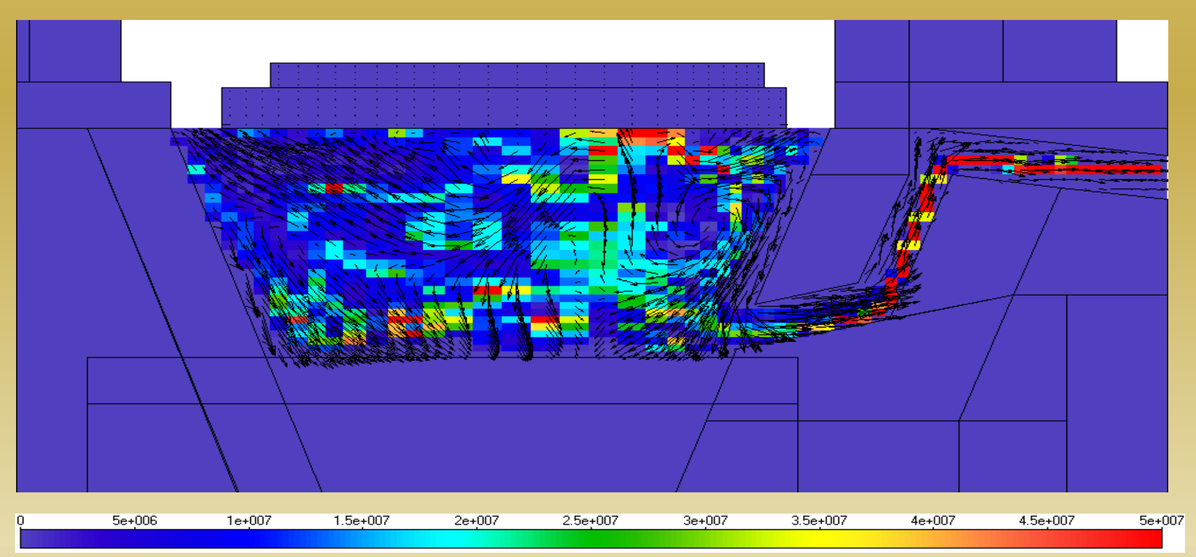

Figure 12-2. Number density (spinel crystals per m^3) in a HLW glass melter (preliminary calculation)

13. Future work

Lab work

- Complete dissolution and growth rate measurement for spinel crystals in molten glass
- Develop a theoretical model for dissolution/growth of spinel crystals under nonisothermal conditions
- Study the dissolution/growth of spinel crystals in periodically increasing and decreasing temperature

Computer work

Compute spinel distribution within the melter and calculate the rate of growth of the spinel sludge bottom layer using the following step-by-step approach.

Step 1

Assumption A1 Spinel crystals enter the melt from the cold cap. Crystals do not change number and size during the process.

Parameters: C and n_s.

Step 2

Assumption A2 Spinel is at equilibrium with molten glass, Equation (3-1).

Parameters: Equilibrium coefficients T_L, B_L, and C_{max} (Section 3); n_s.

Step 3

Assumption A3 Melt redox is a function of T (Section 9) while p_{O_2} is constant (101 kPa). Spinel is at equilibrium with glass as in A2. Redox changes produce oxygen bubbles when the temperature of glass increases. Bubbles affect melt density, and thus influence the temperature and velocity fields.

Parameters: As in A2.

Step 4

Assumption A4 Spinel crystals dissolve and grow (Sections 6 and 7) out of equilibrium in response to T and redox changes.

Parameters: Kinetic coefficients (growth/dissolution rates, D).

Step 5

Assumption A5 Bubble motion and spinel settling produces cellular convection in melt under the cold cap and above the bottom.

Parameters: Spinel fraction fluctuations.

Step 6

Assumption A6 Simulate melter conditions (temperature and flow-through history) for West Valley and Savannah River melters. Compare sludge thickness calculation with measured values.

Parameters: Temperature and flow-through history.

Acknowledgments

Funding for this task was provided by the U.S. Department of Energy Office of Science and Technology. Pacific Northwest National Laboratory is operated for the U.S. Department of Energy by Battelle under Contract DE-AC06-76RLO 1830.

The authors are grateful to Mike Schweiger, Jarrod Crum, and Don Smith for laboratory support and John Vienna for helpful discussions.

We are very sorry to announce that Dr. Alexandr (Sasha) Franěk died as a result of an automobile accident on April 6, 2000. Sasha was a valued member of our team and will be greatly missed both as a friend and a scientific colleague. Sasha was highly qualified in the field of mathematical modeling and contributed significantly to our work.